

## On the Internal Structure of an Adsorption Layer of an Ionic Soluble Surfactant. The Buildup of a Stern Layer Monitored by Optical Means

R. Teppner, K. Haage, D. Wantke, and H. Motschmann\*

Max-Planck-Institute of Colloids and Interfaces, D-14424 Potsdam, Germany

Received: June 16, 2000; In Final Form: September 14, 2000

In the widely accepted Stern model, an adsorption layer of an ionic surfactant at the air–water interface consists of a charged topmost amphiphilic monolayer, a so-called compact Stern layer of directly adsorbed counterions, and the Gouy–Chapman layer characterized by a diffuse ion distribution. The crux of Stern's treatment is the estimation of to what extent ions enter the compact layer and reduce the surface potential. This issue is addressed in this paper by optical means. Surface second harmonic generation, ellipsometry, and surface tension measurements have been used for an investigation of the prevailing ion distribution. Each technique probes different structural elements of the interfacial architecture, and their combination yields a deeper insight into the internal composition of the interface. The amphiphile 1-dodecyl-4-dimethylaminopyridinium bromide, C12-DMP, was used as a cationic soluble surfactant and the comparison with the experimental data obtained with the closely related nonionic betaine 2-(4'-dimethylaminopyridinio)-dodecanoate provided evidence for the correctness of our interpretation of the data. A strikingly different ion distribution with increasing bulk concentration is observed and the underlying mechanism is discussed. Furthermore we are able to clarify the current discussion about the meaning of ellipsometric measurements for adsorption layers of soluble surfactants (with thickness  $< 2$  nm). The dilemma is the impossibility of obtaining on the basis of Fresnel theory (i.e., the solution of Maxwell's equations) a one to one correspondence between measured quantities and the structural data of the monolayer. Commonly it is assumed that ellipsometry measures at least the surface excess but a recent publication questioned this [Teppner et al., *Langmuir* 1999, 15, 7002.]. Our simulations reveal that the effect of optical anisotropy within the layer on the ellipsometric signal is negligible as compared to the effect of a changing ion distribution. This analysis combined with the experimental results on both model systems give us the means to precisely state under which experimental prerequisites ellipsometry directly measures the surface excess as defined by Gibbs.

### 1. Introduction

Electrostatic interactions play a key role for the stabilization of colloidal systems.<sup>2</sup> The repulsive electrical potential between equally charged particles possesses a  $\Phi(r) \propto 1/r$  dependence, where  $r$  is the distance between the particles, and is thus long-ranged. The presence of ions in the solution modifies the potential and leads to a screening of the prevailing interaction as described by the Debye–Hückel theory.<sup>3,4</sup> The long-range interaction is modified by an exponential screening factor  $\Phi(r) \propto e^{-kr}/r$  with  $k$  being proportional to the ionic strength. The assumptions introduced in order to apply Debye–Hückel theory hold as long as the electrostatic potential is small, which is fulfilled at low charge densities and high ion concentrations. Beyond these limits nonlinear effects also become important which can be taken into account at the mean field level by solution of the Poisson–Boltzmann equation.

A particularly interesting problem is the ion distribution next to a charged surface. Ionic amphiphilic molecules form a charged monolayer at the air–water interface and the excess of counterions compensates for the surface charge. The classical model for the interfacial architecture has been derived by Stern, Gouy, and Chapman, although there are some novel approaches which overcome some of the limitations of the classical

theory.<sup>5–7</sup> Gouy and Chapman<sup>8</sup> describe the ion distribution within a diffuse layer by solving the Poisson–Boltzmann equation assuming a homogeneously charged surface and an ion cloud driven by the balance of thermal motion and electrostatic interaction. The model yields the electrostatic potential and the prevailing ion distribution within the diffuse layer. The analysis neglects the physical dimension of the ions and unreasonable results are predicted in the direct vicinity of the charged surface with a high potential  $\Phi_o$ . Stern suggested dividing the counterion distribution into two distinct regions, a compact inner layer of directly adsorbed ions and a diffuse Gouy layer.<sup>9</sup> The crux of this treatment is the estimation of the extent to which ions enter the compact layer and reduce the surface potential.

This problem is tackled in this publication and the prevailing ion distribution is measured by purely optical means. A cationic model system was designed with a headgroup that possesses a sufficiently high hyperpolarizability in order to utilize surface second harmonic generation, SHG.<sup>10</sup> SHG is a nonlinear optical technique of the second order and the signal bears an intrinsic surface specificity which can be easily verified by symmetry considerations.<sup>11,12</sup> In our experiment the SHG signal stems only from the headgroup of the topmost monolayer and allows a determination of the symmetry of the molecular arrangement and the tilt angle of the headgroups as well as the absolute number density of the topmost cationic monolayer.

\* Corresponding author. E-mail: Hubert.Motschmann@mpikg-golm.mpg.de.

Ellipsometry measures changes in the state of polarization upon reflection of a film covered substrate.<sup>13</sup> These changes are linked to the overall reflectivity coefficients of the interface. The problem in interpretation is that the solution of the Maxwell equations does not possess a clear one to one correspondence to the structural data of the monolayer. In the following we try to find an explanation for the surprising nonmonotonic ellipsometric response that depends on the bulk ion concentration published in ref 1, which is replotted here in a different way in Figure 4. First, the effect of changes in the tilt angle with the number density of the anisotropic molecules within the adsorbed layer on the ellipsometric measurements was calculated. It turns out to be insufficient to account for the measurements. Simulations revealed that in case of ionic surfactants the ellipsometric response is strongly affected by the contribution of the diffuse layer. The excess ions within the diffuse layer lead to a refractive index profile with a normal extension of several nm. This concentration profile can be translated into a proper refractive index profile which in turn has a strong impact on the ellipsometric response. Changes in the concentration profile due to the buildup of a Stern layer are well suited to account for the measured effects, whereas the contribution of anisotropy within the layer can be neglected. This analysis enables us to retrieve within the framework of classical theory the total charge of the Stern layer, which means that the formation of the Stern layer can be monitored by purely optical means. To check whether the diffuse layer is responsible for the measured effect, the experimental data obtained with the cationic amphiphile have been compared with the corresponding findings of a closely related amphiphilic betaine. In the betaine both charges are covalently fixed within the headgroup and there is no diffuse layer of ions. The comparison between both model compounds provides further evidence for the correctness of our conclusion.

## 2. Background

**2.1. Ellipsometry Used for the Investigation of Adsorption Layers of Soluble Surfactants.** An ellipsometric experiment measures changes in the state of polarization which occur upon reflection on a film covered support. It yields two quantities,  $\Psi$  and  $\Delta$ , that are related to the ratio of the complex reflectivity coefficients for  $\hat{s}$  and  $\hat{p}$  polarization:<sup>13</sup>

$$\tan \Psi e^{i\Delta} = \frac{r_p}{r_s} \quad (1)$$

The ellipsometric angle  $\Delta$  measures changes in the phase upon reflection, whereas  $\Psi$  probes the reflectivity properties of the sample. Usually a monolayer on a nonabsorbing dielectric support does not change the reflectivity of the sample and hence in the ultrathin film limit only a single quantity is obtained. Unfortunately, the number of independent pieces of data cannot be increased. Simulations reveal that neither spectroscopic ellipsometry<sup>14</sup> nor a variation of the angle of incidence<sup>15,16</sup> yields independent sets of data. All measured quantities remain strongly coupled and the data analysis is restricted to a single quantity, the changes in  $\Delta$ . The reflectivity coefficients of a film covered support can be modeled according to Fresnel (through the solution of Maxwell's equations). For ultrathin films on a support it is convenient to expand the exact formula in a power series of  $h/\lambda$  where  $h$  is the height of the film and  $\lambda$  is the wavelength of light. The first term of the expansion provides a complete description of the optical properties of a monolayer on a support. The ellipsometric experiment then yields a quantity

$d\Delta$  which is proportional to the following integral of the dielectric function  $\epsilon$  across the interfacial region<sup>17</sup>

$$\eta = \int \frac{(\epsilon - \epsilon_1)(\epsilon - \epsilon_2)}{\epsilon} dx \quad (2)$$

where  $\epsilon_1$  and  $\epsilon_2$  are the dielectric constants of the adjacent bulk phases, in our case air and water, respectively. Although optical techniques possess an inherent potential for the characterization of the air–water or oil–water interface, especially the characterization of adsorption layers of soluble surfactants is a tricky business due to the low number density at the interface, the formation of only fairly thin layers (<2 nm) and the prevailing exchange of molecules with the bulk phase. The established way to retrieve surface coverage relies on a proper thermodynamic interpretation of equilibrium surface tension isotherms, a tedious enterprise that demands faster, more convenient, and more accurate alternatives. The advent of such techniques would also be a boost for surface rheology where the determination of the modulus requires second derivatives of the surface tension, which leads to an inherent ambiguity.<sup>18</sup>

Ellipsometry has been proposed as such an alternative.<sup>19,20</sup> In many experiments it is possible to establish from first principles a direct proportionality between the ellipsometric response and surface coverage. If the dielectric constant of the support exceeds those of all other media  $\epsilon_2 \gg \epsilon \approx \epsilon_1$  as is frequently the case for adsorption onto solid supports, the following simplification applies:

$$\eta = \frac{\epsilon_1 - \epsilon_2}{\epsilon_1} \int (\epsilon - \epsilon_1) dx \quad (3)$$

A linear relationship between  $\epsilon$  and the prevailing concentration  $c$  of amphiphile within the adsorption layer is well established (see for instance ref 21)

$$\epsilon = \epsilon_1 + c \cdot \frac{d\epsilon}{dc} \quad (4)$$

This relation yields a direct proportionality between the quantity  $\eta$  and the adsorbed amount  $\Gamma$ .

$$\eta = \frac{\epsilon_1 - \epsilon_2}{\epsilon_1} \cdot \frac{d\epsilon}{dc} \int c dx = \frac{\epsilon_1 - \epsilon_2}{\epsilon_1} \cdot \frac{d\epsilon}{dc} \cdot \Gamma \quad (5)$$

However, none of the assumptions used to derive eq 5 applies for adsorption layers at the liquid–air interface. Drude's equation cannot be further simplified and the relationship between monolayer data and recorded changes remains obscure with no further simplifications possible on the basis of first principles (i.e., solution of Maxwell's equations). The proportionality between the ellipsometric response and the adsorbed amount may hold but must be established by experiment.<sup>22</sup> A recent publication brought the frequently assumed proportionality into question.<sup>1</sup> The ellipsometric isotherm of a cationic soluble amphiphile was measured. The surface tension isotherm resembles all features of a classical soluble surfactant including a critical micelle concentration (cmc). According to Gibbs' fundamental law there is a continuous increase in the surface coverage. However, the ellipsometric response measured in dependence of the bulk concentration showed a pronounced nonmonotonic behavior with a minimum at an intermediate surface concentration. The reason for this feature remained a puzzle but is clarified in this paper. In addition we are now able to make precise predictions under which experimental

requisites the surface excess can directly be retrieved by ellipsometry.

**2.2. Adsorption Layers Formed by Soluble Ionic Surfactants.** The ion distribution in the diffuse layer is given by the solution of the Poisson equation which relates the divergence of the gradient of the electric potential  $\Phi$  to the charge density  $\rho$  at that point (see for instance ref 4):

$$\text{div grad}\Phi = \Delta\Phi = -\frac{\rho}{\epsilon_0\epsilon_r} \quad (6)$$

The topmost monolayer of the cationic amphiphile is positively charged and in contact with an electrolyte solution which forms a diffuse layer of charges. The ion concentration distribution within the electrical potential  $\Phi$  is given by Boltzmann:

$$c^- = c_o^- e^{z^-e\Phi/k_B T} \quad c^+ = c_o^+ e^{-z^+e\Phi/k_B T} \quad (7)$$

where  $z^-$  and  $z^+$  are the valencies of the anions and cations, respectively. For a symmetric electrolyte solution ( $-z^- = z^+ = z$  and  $c_o^- = c_o^+ = c_o$ ) eq 7 leads to a net charge of the ion cloud of

$$\rho = ze(c^+ - c^-) = -2c_o ze \sinh\frac{ze\Phi}{k_B T} \quad (8)$$

The combination of eq 8 with the Poisson equation (eq 6) yields a differential equation in the electric potential  $\Phi$ . In our case the potential is only a function of the normal coordinate to the surface  $x$ . It is convenient to define a reduced potential

$$y = \frac{ze\Phi}{k_B T} \quad y_o = \frac{ze\Phi_o}{k_B T} \quad (9)$$

that further simplifies the equations and results in

$$\frac{d^2y}{dx^2} = \frac{2c_o z^2 e^2}{k_B T \epsilon_0 \epsilon_r} \sinh y = k^2 \sinh y \quad (10)$$

The integration of eq 10 with the boundary conditions ( $y = 0$  and  $dy/dx = 0$ ) for  $x = \infty$  and  $y = y_o$  at  $x = 0$  lead to the Gouy–Chapmann solution of the reduced potential within the diffuse layer:

$$e^{y/2} = \frac{e^{y_o/2} + 1 + (e^{y_o/2} - 1)e^{-kx}}{e^{y_o/2} + 1 - (e^{y_o/2} - 1)e^{-kx}} \quad (11)$$

The Gouy–Chapman model provides unreasonable results in the direct vicinity of the interface provided that  $\Phi_o$  is large. One reason is the model's use of point charges and the neglect of the physical dimensions of the ions. Stern bridged this gap by a division of the interfacial layer in two distinct regions, a layer of directly bound ions and a diffuse Gouy layer. The difficulty of Stern's division is an experimental or theoretical determination of the individual isotherm corresponding to the ion content of diffuse and compact layer.

### 3. Experimental Section

**Materials.** The chemical formula of the soluble cationic amphiphile 1-dodecyl-4-dimethylaminopyridinium bromide, C12-DMP bromide, used in this study is presented in Figure 1. The SHG activity is provided by the cationic headgroup with the dimethyl amino group  $N(\text{CH}_3)_2$  acting as an electron donor. For an identification of the influence of the ion distribution on the

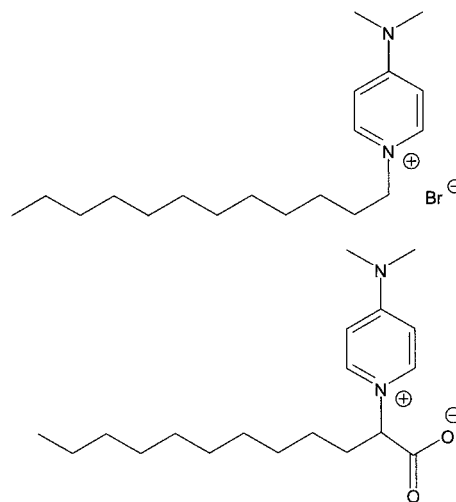


**Figure 1.** Chemical structures of the cationic amphiphile 1-dodecyl-4-dimethylaminopyridinium bromide, C12-DMP bromide, and the closely related nonionic 2-(4-dimethylaminopyridinio)-dodecanoate, C12-DMP betaine.

ellipsometric isotherm the betain 2-(4-dimethylaminopyridinio)-dodecanoate, C12-DMP betaine, was used. Details about the synthesis, analysis, and various physical properties can be found in ref 23.

**Sample Preparation.** An aqueous solution of the surfactant at a concentration close to the critical micelle concentration was prepared using bidistilled water. This solution was then purified using a fully automated device described in ref 24. The applied purification scheme ensures a complete removal of any surface active impurities by repeated cycles of (a) compression of the surface layer, (b) its removal with the aid of a capillary, (c) dilation to an increased surface area, and (d) again a formation of a new adsorption layer. These cycles are repeated until the equilibrium surface tension  $\sigma_e$  between subsequent cycles remains constant, which indicates that all surface active trace impurities that might have an impact on the measurements are completely removed. Solutions of different concentrations were prepared by a dilution of the stock solution.

**Surface Tension Measurement.** With a ring tensiometer (model K10, Krüss) the surface tension was recorded until a constant equilibrium value,  $\sigma_e$ , was established. The critical micelle concentration was determined on the basis of the adsorption isotherm. The cmc values of the members of the homologous series strictly follow the Stauff–Klevens equation.<sup>25</sup> The cationic  $C_{12}$  compound has a cmc of  $4.31 \times 10^{-3}$  mol/L.

**Conductivity.** The activity coefficient was determined by conductivity measurements. These measurements were performed on a microprocessor conductivity meter (WTW-LF537; electrode: WTW TetraCon96) at 298 K.

**Second Harmonic Generation.** Second harmonic generation experiments were carried out in reflection mode at a fixed angle of incidence of  $53^\circ$ . The fundamental ( $\lambda = 1064$  nm) of an active-passive mode locked Nd:YAG laser (PY-61, Continuum) with a pulse width of  $\tau = 30$  ps and a repetition rate of 12.5 Hz was used as a light source. All spurious SHG created by the optical components were removed by a visible cutoff filter (RG630, Schott) placed just in front of the sample. The frequency doubled light generated at the interface was separated from the fundamental using an IR-cutoff filter (BG39, Schott) in conjunction with a narrow band interference filter (532 BP, Instruments S. A.) and subsequently detected by a photomultiplier (C83068, Burle) with a quantum efficiency of 15%. The signal was amplified (V5D, Seefeldler Messtechnik) and pro-

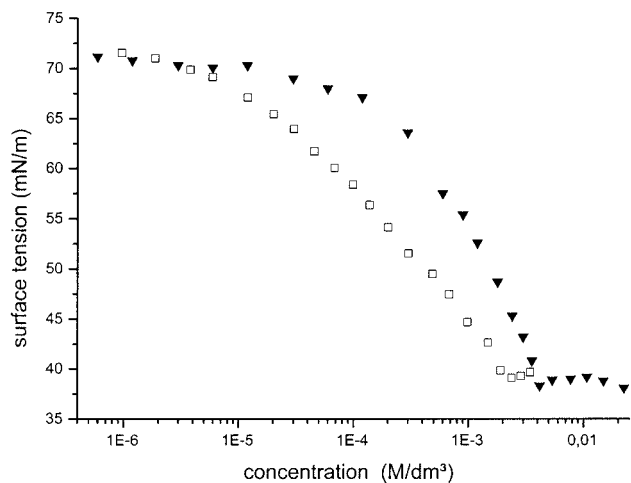


**Figure 2.** The equilibrium surface tension  $\sigma_e$  of a purified aqueous solution of the ionic C12-DMP bromide (triangles) and the nonionic C12-DMP betaine (squares) as a function of the bulk concentration  $c_0$ .

cessed by a 500 MHz, 2 Gs/s digitizing oscilloscope (HP 54522 A, Hewlett Packard). A computer controlled all vital elements of the experiment and performed the integration of the waveform. The SHG signal of a quartz crystal was used as a reference in order to eliminate experimental errors due to intensity fluctuations. The plane of polarization of the incident beam can be rotated by a Glan laser polarizer (extinction ratio  $10^{-6}$ , PGL, Halle) and a low order quartz half-wave plate ( $\Delta\lambda = 0.001$ , RLQ Halle) mounted on motor driven, computer controlled rotary stages (M-445.21, Physik Instruments). The polarization of the reflected SHG-light was analyzed using a Glan-Thomson prism (extinction ratio  $10^{-6}$ , Type K, Steeg & Reuter).

**Ellipsometry.** All relevant design features of the ellipsometer (Multiskop, Optrel) are discussed in detail in ref 26. We used the Null ellipsometer mode of the ellipsometry module in a laser, polarizer, compensator, sample, analyzer arrangement at an angle of incidence of  $56^\circ$ .

#### 4. Results and Discussion

The experimental surface tension isotherms (surface tension  $\sigma_e$  versus bulk concentration) of both amphiphilic model compounds are presented in Figure 2. The solid triangles refer to the cationic amphiphile C12-DMP bromide and the hollow squares to the nonionic C12-DMP betaine. Surface active impurities, a major concern for this study,<sup>27,28</sup> have been removed by extended purification as referenced above. The experimental isotherm allows a determination of the total surface excess according to Gibbs' fundamental law:

$$\Gamma = -\frac{1}{mRT} \cdot \frac{d\sigma_e}{d \ln a} \approx -\frac{1}{mRT} \cdot \frac{d\sigma_e}{d \ln c} \quad (12)$$

where the factor  $m$  accounts for the contribution of anions and cations.

The members of the homologous series of the alkyl-dimethylaminopyridinium bromide are strong electrolytes and follow the predictions of Debye-Hückel theory. This has been experimentally verified by conductivity measurements. For solubility reasons we used 1-butyl-4-dimethylaminopyridinium bromide instead of the  $C_{12}$  representative of the homologous series which gave us experimental access to a wider concentration range. Debye-Hückel theory predicts a proportionality of the activity coefficient to the square root of the ionic strength

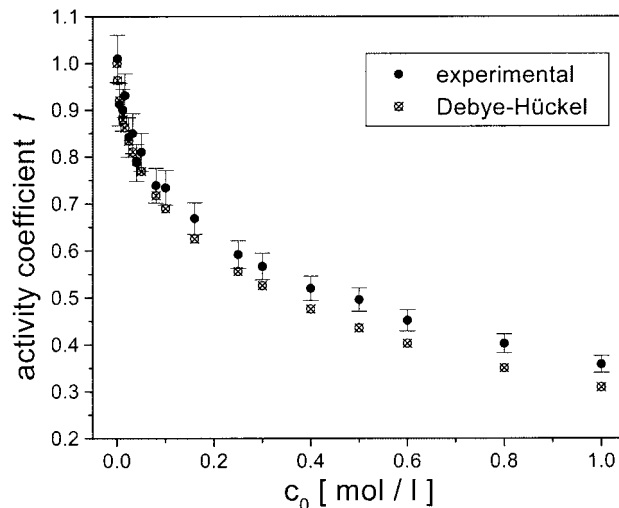


**Figure 3.** The activity coefficient  $f$  retrieved from conductivity measurements and predicted by Debye-Hückel theory of an aqueous solution of 1-butyl-4-dimethylaminopyridinium bromide as a function of the bulk concentration  $c_0$ .

for aqueous solutions of 1:1 electrolytes which is indeed observed in our experiment.

$$\log f_{\pm} = -0.5909\sqrt{I} \quad (13)$$

The experimental activity coefficients are presented in Figure 3 together with the results obtained by Debye-Hückel theory.

The number density of cationic amphiphiles within the topmost monolayer has been measured by SHG. The headgroup of the surfactant possesses a sufficiently high hyperpolarizability  $\beta$  and is the only structural element being picked up by SHG. In our case the SHG signal is determined by the dipolar contribution and combinations of various components of the macroscopic susceptibility tensor  $x^{(2)}$  are measured within a reflection experiment. The relation between the elements of the macroscopic susceptibility tensor  $x^{(2)}$  and the corresponding molecular quantities is provided by the oriented gas model:<sup>29,30</sup>

$$x^{(2)} \propto \sum_{\text{mol}} \beta \propto N \langle \beta \rangle \quad (14)$$

It states that the susceptibility  $x^{(2)}$  is the sum of the hyperpolarizabilities  $\beta$  of all molecules. Alternatively this can be expressed in terms of the number density of the SHG active molecules,  $N$ , and the corresponding orientational average  $\langle \beta \rangle$  as denoted by the brackets. An evaluation of the SHG intensity bears information on the number density  $N$  at the interface and the ratio between certain susceptibility elements yields the mean orientation of the headgroup.<sup>31</sup> Since the orientational average of  $\beta$  vanishes in the bulk the signal is only sensitive to the topmost monolayer.

Details on the data analysis can be found in ref 32. The main findings are (a) the orientational order of the headgroup is independent of the surface coverage with a tilt angle of  $49^\circ$  of the long chromophore axis with respect to the surface normal; (b) the symmetry of the molecular arrangement of the headgroup belongs to the point group  $C_{\infty v}$ , which is characterized by an isotropic azimuthal arrangement within the adsorption layer.

The absolute number density of the cationic amphiphile within the topmost monolayer was determined by an evaluation of the intensity of a properly calibrated SHG signal. For the purpose of calibration we used a Langmuir layer of the water insoluble  $C_{20}$  representative of the homologous series. The number density

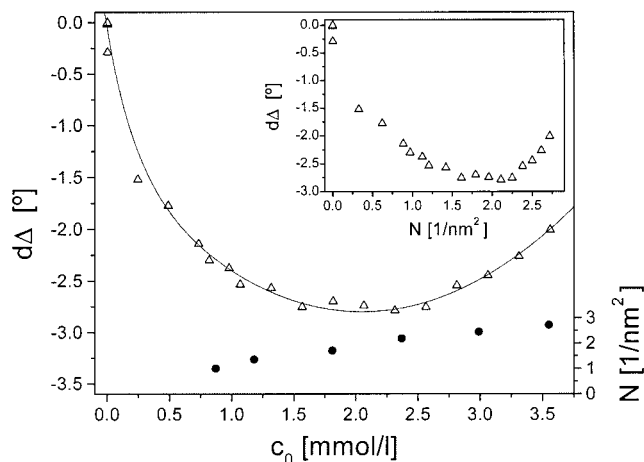


**Figure 4.** The ellipsometric quantity  $d\Delta$  (triangles with the solid line being a guide to the eye) decreases at low surface coverage with the concentration of the solution and shows a minimum at an intermediate concentration far below the cmc, whereas the number density  $N$  of molecules within the topmost layer (circles), measured by SHG, increases monotonically. The inset shows the nonmonotonic dependence of  $d\Delta$  on  $N$ .

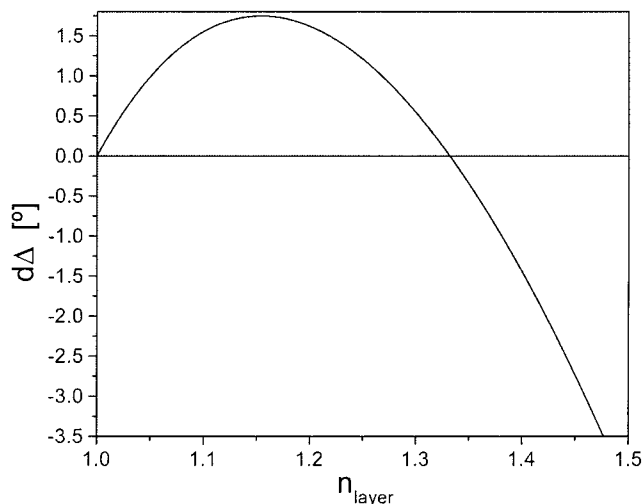
of a quasi two-dimensional Langmuir layer is directly given by the preparation and also all effects and complications which might arise from local field corrections are intrinsically taken into account.

Figure 4 shows the number of molecules as determined by SHG in dependence of the bulk concentration. As expected the number density  $N$  increases in a monotonic fashion. These data yield the charge density produced by the cationic amphiphilic monolayer at the interface.

The ellipsometric isotherm is presented in Figure 4 in a linear scale; the triangles refer to the measured ellipsometric values below the cmc. A remarkable feature is the high sensitivity at submonolayer coverage and the pronounced minimum in the ellipsometric isotherm at an intermediate bulk concentration. Obviously the ellipsometric signal has a complex nonmonotonic relation with the bulk concentration. Commonly it was assumed that ellipsometry at least measures the surface excess as defined by Gibbs. The inset of Figure 4, which is replotted from ref 1, demonstrates that this need not necessarily be the case and leads to the preliminary conclusion that ellipsometry, although valuable to monitor qualitative changes in surface coverage, is not a suitable technique to quantify the surface excess. In the following, simulations are presented that were performed in an attempt to explain the ellipsometric isotherm. All of those calculations were done for a wavelength of  $\lambda = 632.8$  nm and an angle of incidence of  $\phi = 56^\circ$  according to the ellipsometric setup. The results make the preliminary conclusion more precise.

**Scenario 1: Filling up the Adsorption Layer.** The adsorption layer is described as an isotropic optical layer of constant thickness with a refractive index  $n_{\text{layer}}$  which depends on the surface coverage.<sup>33</sup> Within this model there are two distinct surface concentrations which lead to a vanishing  $d\Delta = \Delta - \Delta_0 = 0^\circ$ . At very low coverage the refractive index of the layer matches the one of air  $n_{\text{layer}} = n_{\text{air}} = 1$  and at an intermediate surface coverage the surface layer adopts the very same refractive index as the water bulk phase  $n_{\text{layer}} = n_{\text{water}} = 1.332$ . Consequently there is an extremum in between. The resulting  $d\Delta(n_{\text{layer}})$  curve is depicted in Figure 5. The dimension of the molecules has been used as thickness of the layer.

Obviously this scenario is not suitable to explain the measurement, since  $d\Delta_{\text{max}} \approx 1.75^\circ$  has even the wrong sign!



**Figure 5.** Simulation of the effect of a changing refractive index of a layer of constant thickness  $d = 2.1$  nm on the ellipsometric signal  $d\Delta$ .

The experimental data require  $n_{\text{layer}} > n_{\text{water}}$  at all concentrations. Hence water instead of air is the effective environment of the adsorption layer.

**Scenario 2: Effect of Anisotropy.** The aim of this investigation was to address the impact of a change of the molecular tilt on the ellipsometric angles. The following assumptions were made to estimate an upper limit for this effect:

(i) The optical model is that of a uniaxial layer with the optical axis normal to the interface. The molecular arrangement is  $C_{\infty V}$  which has been experimentally verified by polarization dependent SHG measurements for the headgroups.

(ii) The thickness of the adsorbed layer and the mean tilt angle of the molecules within the layer change with their number density  $N$  at the interface. Within the investigated number density range the thickness increases from 1 to 1.9 nm proportional to the cosine of the tilt angle which is assumed to change from around  $70^\circ$  to  $40^\circ$ .

(iii) The whole molecule, including the headgroup, is assumed to change its tilt angle. The molecules are assumed to be all-trans and perfectly aligned which would yield the maximum possible change in anisotropy.

(iv) The refractive index for an  $E$ -vector along the length axis of the molecule is  $n_{\text{axis}} = 1.56$ , which is the maximum value for a densely packed layer. The effective refractive index of the layer for an  $E$ -vector oscillating in this direction is dependent on the volume concentration of the molecules within the layer. The refractive index for an  $E$ -vector perpendicular to the long axis of the molecule is  $n_{\text{perp}} = 1.48$  for a dense and perfectly oriented layer. The effective refractive index again is dependent on the prevailing volume concentration. Both refractive indices have been taken from Riegler et al.<sup>34</sup> and rely on a combination of X-ray reflection data with ellipsometric measurements of monolayers of behenic acid at the air-water interface.

The calculated  $d\Delta(N)$  versus density curve is plotted in Figure 6. Obviously a change of the molecular tilt leads to changes in  $d\Delta$  but cannot account for the measured pronounced extremum. In addition it is impossible to reach  $d\Delta = -2.77^\circ$ , which is the minimum of the measured curve, with reasonable parameters for the anisotropic layer. An increase in the anisotropy has the same impact on the ellipsometric measurements as a reduction of the layer thickness; hence, the only way to get closer to  $d\Delta = -2.77^\circ$  is to diminish the anisotropy!

At this point we would like to point out that the assumptions made for this simulation exaggerate the anisotropy effect. The

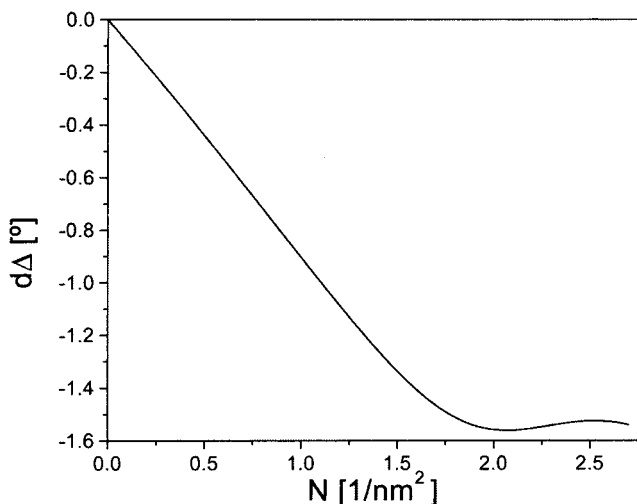


**Figure 6.** Investigation of the impact of anisotropy on the ellipsometric signal. The ellipsometric signal  $d\Delta$  calculated in dependence of the number density of adsorbed molecules  $N$ . A molecular length of 2.1 nm and a refractive index of  $n_{axis} = 1.56$  for an  $E$ -vector along and of  $n_{perp} = 1.48$  for an  $E$ -vector perpendicular to the molecular axis were used. The layer thickness (1.0 to 1.9 nm), the tilt angle ( $70^\circ$  down to  $40^\circ$ ),  $n_s$  and  $n_p$  were all assumed to be dependent on the surface coverage.

SHG measurements reveal that the heads do not change their tilt angle at all. This means that only the tails may change their tilt, which results in an even thinner anisotropic layer and therefore a smaller effect. Additionally the tails are certainly neither all-trans nor perfectly oriented even at the highest coverage measured which corresponds to a molecular area of  $0.37 \text{ nm}^2$  (see for example ref 35). For these reasons Figure 6 represents an upper limit of the impact of anisotropy. The real effect is smaller by far for the surface coverages encountered here, which means that anisotropy cannot account for the surprising feature of the ellipsometric isotherm. This result is in contradiction to ref 1, because the latter did not account for the changing surface coverage.

**Scenario 3: Changing the Counterion Distribution.** The aim of this analysis is to describe the maximum in the ellipsometric data in terms of a contribution of the counterions. Ellipsometry probes the complete interfacial architecture; and

the reflected light is generated within the transition region between both adjacent bulk phases, the air and the aqueous surfactant solution.

As already outlined, the surface charge of the cationic amphiphilic monolayer is compensated by the counterions as described by Gouy–Chapman. The optical analysis requires the translation of the prevailing distribution of molecules and ions within the interphase into a corresponding refractive index profile. The reflectivity coefficients can then be calculated on the basis of numerical algorithms developed for stratified media.<sup>17</sup> Two elements dominate the refractive index profile and hence the reflectivity properties, the topmost monolayer of the amphiphile and the distribution of ions within the diffuse layer. The excess of ions within the diffuse layer leads to a slightly elevated refractive index as compared to the bulk of the aqueous surfactant solution. The typical dimensions of the diffuse layer are on the order of 10 nm and this fairly wide extension leads to a profound impact on  $\Delta$ . The solution of the potential  $\Phi$  plugged into eq 8 yields the distribution of anions and cations within the diffuse layer. The prevailing charge distribution is determined by the surface charge of the topmost monolayer. The refractive index profile is then determined by the ion distribution by a multiplication with the refractive index increment  $dn/dc$  which has been independently measured with an Abbe refractometer. Figure 7 sketches the model for the interface. At lower surface coverage most of the ions are spread out within the diffuse layer leading to a pronounced refractive index profile. This situation is sketched in Figure 7a. At higher concentrations some ions enter the adsorption layer and form ion pairs with the headgroups accounted for with a lower  $dn/dc$  value as compared to the bulk phase. The formation of this Stern layer effectively reduces the surface charge and as a consequence the extension and the magnitude of the refractive index profile of the diffuse layer decrease. This is sketched in Figure 7b.

This model has been used for monitoring the formation of the Stern layer. The ion distribution within the diffuse layer is determined by the total effective charge density at the interface. The SHG measurements yield the number density and charge density produced by the cationic amphiphilic monolayer. The effective charge density at the interface is given by this value reduced by the number density of counterions within the Stern

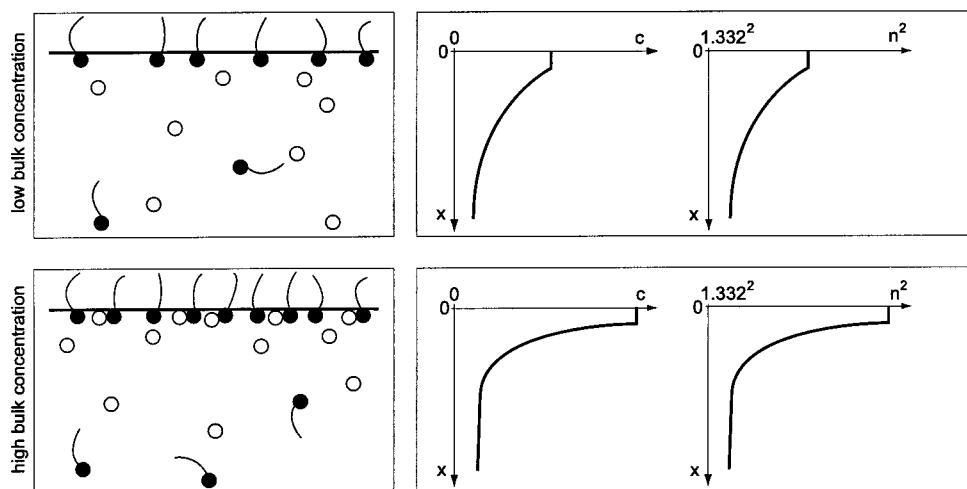


**Figure 7.** The interphase of a soluble surfactant at the air–water interface consists of a charged topmost cationic monolayer, a compact layer of directly adsorbed counterions and the diffuse layer of counterions. The charge density of the topmost monolayer reduced by the charge of the inner Stern layer determines the ion distribution within the diffuse layer. The prevailing ion distribution is given by solution of the nonlinear Poisson–Boltzmann equation. The excess of ions can be readily translated in the corresponding refractive index profile. The profile determines the reflectivity properties. Ellipsometric data modeled within this framework allow an estimation of the extent to which ions enter the compact layer.

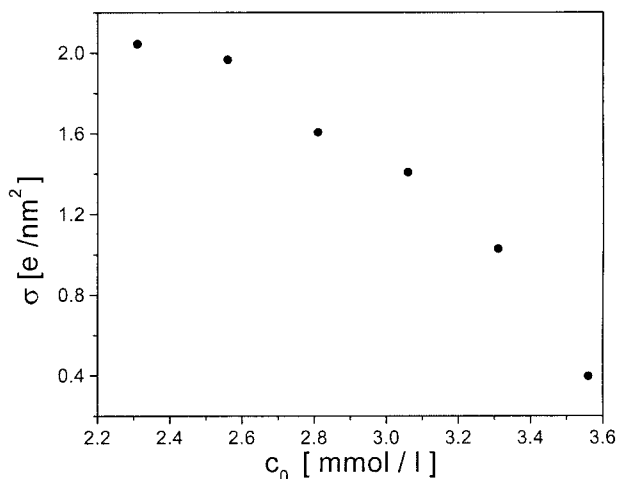


**Figure 8.** The charge density of the topmost monolayer has been retrieved by optical means. The surface charge refers to the number density of the cationic amphiphile reduced by the number of ions within the Stern layer.

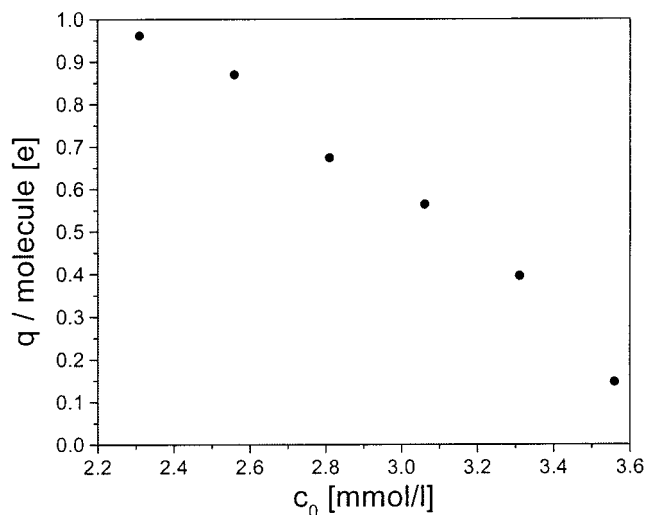


**Figure 9.** Decreasing mean specific charge per adsorbed C12-DMP molecule due to the build-up of the Stern layer of counterions as computed from SHG and ellipsometric data.

layer. The corresponding refractive index of Stern and topmost monolayer is given by an effective medium approach. Hence the optical properties of the monolayer are known by independent means. Furthermore the refractive index profile of the diffuse layer is given once the effective charge density at the interface is known. We used the experimental data in order to retrieve the corresponding effective surface charge density. The results are depicted in Figure 8 starting in the vicinity of the extremum of the ellipsometric isotherm. Since the number density of amphiphilic molecules within the adsorbed layer is known, this can also be plotted as the specific charge per adsorbed molecule depending on the bulk ion concentration (Figure 9). Hence, with this model we are able to monitor by purely optical means the extent to which ions enter the compact Stern layer.

If the minimum in the ellipsometric isotherm is the result of different ion distributions at different bulk concentrations and simply reflects that ions do enter the compact layer, then no minimum should be observed in the case of the absence of a diffuse layer. For this reason we carried out the same investigation with the closely related C<sub>12</sub>-DMP betaine. In the betaine both charges are covalently bound within the same molecule. The headgroup just acts as a dipole, and consequently no diffuse

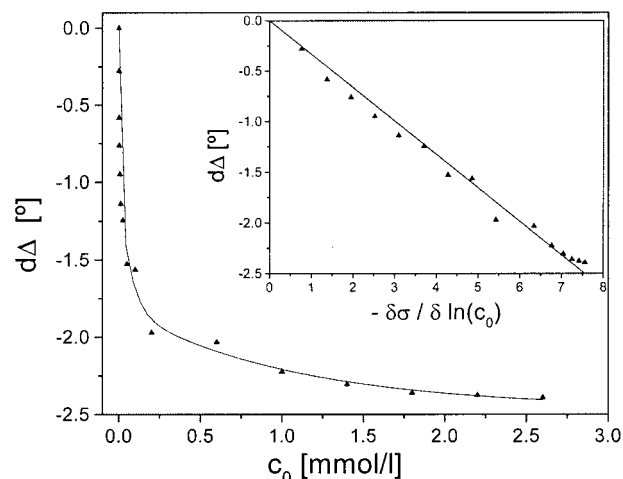


**Figure 10.** Ellipsometric isotherm of the nonionic C12-DMP betaine. The ellipsometric isotherm decreases in a monotonic fashion and is proportional to the surface excess. The inset compares the surface excess according to Gibbs and the ellipsometric response.

layer is produced. The corresponding ellipsometric isotherm is shown in Figure 10. The ellipsometric signal changes in a monotonic fashion and reaches a limiting value at the cmc. The inset compares the surface excess retrieved by an analysis of the isotherm according to Gibbs' fundamental law with the corresponding ellipsometric data; the proportionality is evident. The comparison reveals that the surface excess of nonionic soluble surfactants can be directly measured by ellipsometry. In all other cases the prevailing ion distribution has to be considered, whereas the anisotropy of the adsorption layer can be neglected for such small surface coverages.

## 5. Summary and Conclusion

The internal structure of an adsorption layer of a cationic soluble amphiphile has been monitored by ellipsometry and surface second harmonic generation. The data have been interpreted in terms of the widely accepted Stern–Gouy–Chapman model which divides the counterion distribution in a compact layer of directly adsorbed ions and a diffuse layer. The combination of both optical techniques is sensitive to the prevailing ion distribution. The extent to which ions enter the Stern layer can be retrieved by optical means. Furthermore the experimental data and the corresponding analysis suggest that the surface excess of nonionic surfactants can be directly measured by ellipsometry. It is also demonstrated that anisotropy has only a minor impact on the ellipsometric response. A comparison of our ionic model compound with a closely related nonionic betaine supports this conclusion. The interpretation of our data remains in the framework of Stern–Gouy–Chapman although some recent theoretical papers dispute this.<sup>36,37</sup> Monte Carlo simulations of the prevailing ion distributions are currently being performed.

**Acknowledgment.** The authors thank Prof. H. Möhwald, Dr. R. Netz, and A. Moreira for stimulating discussions.

## References and Notes

- (1) Teppner, R.; Bae, S.; Haage, K.; Motschmann, H. *Langmuir* **1999**, *15*, 7002.
- (2) Evans, D. F.; Wennerström, H. *The Colloidal Domain*; VCH Publishers: New York, 1994.
- (3) Debye, P. W.; Hückel, E. *Z. Phys.* **1923**, *24*, 185.
- (4) Adamson, A. W. *Physical Chemistry of Surfaces*; Wiley & Sons: New York, 1993.

- (5) Marcelja, S. *Langmuir* **2000**, *16*(15), 6081–6083.
- (6) Parsegian, V. A.; Evans, E. A. *Curr. Opin. Colloid Interface Sci.* **1996**, *1*(1), 53–60.
- (7) Kjellander, R.; Ulander, J. *Journal de Physique IV* **2000**, *10*(P5), 431–436.
- (8) Gouy, G. *J. Phys.* **1910**, *9*(4), 457. Chapman, D. L. *Philos. Mag.* **1913**, *25*(6), 475.
- (9) Stern, O. *Z. Elektrochem.* **1924**, *30*, 508.
- (10) Bae, S.; Haage, K.; Wantke, K.; Motschmann, H. *J. Phys. Chem. B* **1999**, *103*, 1045.
- (11) Shen, Y. R. *Annu. Rev. Phys. Chem.* **1989**, *40*, 327.
- (12) Corn, R. M.; Higgins, D. A. *Chem. Rev.* **1994**, *94*, 107.
- (13) Azzam, R. M.; Bashara, N. M. *Ellipsometry and Polarized Light*; North-Holland Publication: Amsterdam, 1979.
- (14) Reiter, R.; Motschmann, H.; Orendi, H.; Nemetz, A.; Knoll, W. *Langmuir* **1992**, *8*, 1784.
- (15) Ayoub, G. T.; Bashara, N. M. *J. Opt. Soc. Am.* **1978**, *68*, 978.
- (16) Dignam, M. J.; Moskowitch, M.; Stobie, R. W. *Trans. Faraday Soc.* **1971**, *67*, 3306.
- (17) Lekner, J. *Theory of Reflection*; Martinus Nijhoff Publishers: Boston, 1987.
- (18) Wantke, K. D.; Fruhner, H.; Fang, J. P.; Lunkenheimer, K. *J. Colloid Interface Sci.* **1998**, *208*(1), 34–48.
- (19) Bain, C. D. *Curr. Opin. Colloid Interface Sci.* **1998**, *3*, 287.
- (20) Möbius, D. *Curr. Opin. Colloid Interface Sci.* **1996**, *1*, 250.
- (21) Motschmann, H.; Stamm, M.; Toprakcioglu, C. *Macromolecules* **1991**, *24*, 3681.
- (22) Hutchison, H.; Klenerman, S.; Manning-Benson, S.; Bain, C. *Langmuir* **1999**, *15*, 7530.
- (23) Haage, K.; Motschmann, H.; Bae, S.; Grndemann, E. *J. Colloid Interface Sci.* (submitted).
- (24) Lunkenheimer, K.; Pergande, H. J.; Krüger, H. *Rev. Sci. Instrum.* **1987**, *58*, 2313.
- (25) Stauff, J. *Kolloidchemie*; Springer: Berlin, 1960.
- (26) Harke, M.; Teppner, R.; Schulz, O.; Orendi, H.; Motschmann, H. *Rev. Sci. Instr.* **1997**, *68*(8), 3130.
- (27) Elworthy, P. H.; Mysels, K. J. *J. Colloid Interface Sci.* **1966**, 331.
- (28) Lunkenheimer, K. *J. Colloid Interface Sci.* **1989**, *131*, 580.
- (29) Motschmann, H.; Penner, T.; Armstrong, N.; Enzenyilimba, M. *J. Phys. Chem.* **1993**, *97*, 3933.
- (30) Prasad, P.; Williams, D. J. *Introduction to Nonlinear Optical Effects in Molecules and Polymers*; Wiley: New York, 1991.
- (31) Harke, M.; Ibn Elhaj, M.; Möhwald, H.; Motschmann, H. *Phys. Rev. E* **1998**, *57*, 1806.
- (32) Bae, S.; Haage, K.; Wantke, D.; Motschmann, H. *J. Phys. Chem. B.* **1999**, *103*(7), 1045.
- (33) Pfohl, T.; Möhwald, H.; Riegler, H. *Langmuir* **1998**, *14*, 5285.
- (34) Paudler, M.; Ruths, J.; Riegler, H. *Langmuir* **1992**, *8*, 184.
- (35) Aveyard, R.; Carr, N.; Slezok, H. *Can. J. Chem.* **1985**, *63*, 2742.
- (36) Netz, R. *Phys. Rev. E* **1999**, *60*, 3174.
- (37) Netz, R. *Europhysics. Lett.* **1999**, *45*, 726.